



1 **Geochemistry of the dissolved loads of rivers in Southeast Coastal Region, China:**

2 **Anthropogenic impact on chemical weathering and carbon sequestration**

3 Wenjing Liu<sup>1,2,3</sup>, Zhifang Xu<sup>1,2,3\*</sup>, Huiguo Sun<sup>1,2,3</sup>, Tong Zhao<sup>1,2,3</sup>, Chao Shi<sup>1,2</sup>, Taoze Liu<sup>4</sup>

4 <sup>1</sup> Key Laboratory of Cenozoic Geology and Environment, Institute of Geology and

5 Geophysics, Chinese Academy of Sciences, Beijing 100029, China

6 <sup>2</sup> Institutions of Earth Science, Chinese Academy of Sciences, Beijing 100029, China

7 <sup>3</sup> University of Chinese Academy of Sciences, Beijing 100049, China

8 <sup>4</sup> State Key Laboratory of Environmental Geochemistry, Institute of Geochemistry, Chinese

9 Academy of Sciences, Guiyang, Guizhou 550002, China

10 \* Corresponding author. [zfxu@mail.igcas.ac.cn](mailto:zfxu@mail.igcas.ac.cn) (Zhifang Xu, Tel: +86 10 82998289)



11 **Abstract:**

12 Southeast coastal region is the most developed and populated area in China.

13 Meanwhile, it has been the most severe acid rain impacted region for many years. The

14 chemical compositions and carbon isotope ratio of dissolved inorganic carbon

15 ( $\delta^{13}\text{C}_{\text{DIC}}$ ) of rivers were investigated to evaluate the chemical weathering and

16 associated atmospheric  $\text{CO}_2$  consumption rates. Mass balance calculation indicated

17 that the dissolved loads of major rivers in the Southeast Coastal Rivers Basin

18 (SECRB) were contributed by atmospheric (14.4%, 6.6-23.4%), anthropogenic

19 (17.8%, 0-55.2%), silicate weathering (38.3%, 10.7-74.0%) and carbonate weathering

20 inputs (29.4%, 3.9-62.0%). The silicate and carbonate chemical weathering rates for

21 these river watersheds were  $10.0\text{-}29.6 \text{ t km}^{-2} \text{ a}^{-1}$  and  $1.0\text{-}54.1 \text{ t km}^{-2} \text{ a}^{-1}$ , respectively.

22 The associated mean  $\text{CO}_2$  consumption rate by silicate weathering for the whole

23 SECRB were  $167 \times 10^3 \text{ mol km}^{-2} \text{ a}^{-1}$ . The chemical and  $\delta^{13}\text{C}_{\text{DIC}}$  evidences indicated

24 that sulfuric acid (mainly from acid deposition) was significantly involved in chemical

25 weathering of rocks. The calculation showed an overestimation of  $\text{CO}_2$  consumption

26 at  $0.19 \times 10^{12} \text{ g C a}^{-1}$  if sulfuric acid was ignored, which accounted for about 25% of

27 the total  $\text{CO}_2$  consumption by silicate weathering in the SECRB. This study

28 quantitatively highlights that the role of sulfuric acid in chemical weathering,

29 suggesting that acid deposition should be considered in studies of chemical

30 weathering and associated  $\text{CO}_2$  consumption.

31 **Keywords:** Southeast Coastal Rivers Basin; Chemical weathering;  $\text{CO}_2$  consumption;

32 acid deposition;



## 33 1. Introduction

34 Chemical weathering of rocks is a key process that links geochemical cycling of  
35 solid earth to the atmosphere and ocean. It provides nutrients to terrestrial and marine  
36 ecosystems and regulates the level of atmospheric CO<sub>2</sub>. As a net sink of atmospheric  
37 CO<sub>2</sub> on geologic timescales, estimation of silicate chemical weathering rates and the  
38 controlling factors are important issues related to long-term global climate change  
39 (e.g. Raymo and Ruddiman, 1992; Négrel et al. 1993; Berner and Caldeira, 1997;  
40 Gaillardet et al., 1999; Kump et al., 2000; Amiotte-Suchet et al., 2003; Oliva et al.,  
41 2003; Hartmann et al., 2009; Moon et al., 2014). As an important component in the  
42 Earth's Critical Zone (U.S. Nat. Res. Council Comm., 2001), river serves as an  
43 integrator of various natural and anthropogenic processes and products in a basin, and  
44 a carrier transporting the weathering products from continent to ocean. Therefore, the  
45 chemical compositions of river are widely used to evaluate chemical weathering and  
46 associated CO<sub>2</sub> consumption rates at catchment and/or continental scale, and examine  
47 their controlling factors (e.g., Edmond et al., 1995; Gislason et al., 1996; Galy and  
48 France-Lanord, 1999; Huh, 2003; Millot et al., 2002, 2003; Oliva et al., 2003; West et  
49 al., 2005; Moon et al., 2007; Noh et al., 2009; Shin et al., 2011; Calmels et al., 2011).

50 With the intensification of human activities, human perturbations to river basins  
51 have increased in frequency and magnitude. It is important to understand how such  
52 perturbations function on the current weathering systems and to predict how they will  
53 affect the Critical Zone of the future (Brantley and Lebedeva, 2011). In addition to  
54 CO<sub>2</sub>, other sources of acidity (such as sulfuric, nitric and organic acids) can also



55 produce protons. These protons react with carbonate and silicate minerals, thus  
56 enhance rock chemical weathering rate and flux compared with only considering  
57 protons deriving from CO<sub>2</sub> dissolution (Calmels et al., 2007; Xu and Liu, 2010). The  
58 effect of other sourced proton (especially H<sup>+</sup> induced by SO<sub>2</sub> and NO<sub>x</sub> coming from  
59 anthropogenic activities) on chemical weathering is documented to be an important  
60 mechanism modifying atmospheric CO<sub>2</sub> consumption by rock weathering (Galy and  
61 France-Lanord, 1999; Semhi, et al., 2000; Spence and Telmer, 2005; Xu and Liu,  
62 2007; Perrin et al., 2008; Gandois et al., 2011). Anthropogenic emissions of SO<sub>2</sub> was  
63 projected to provide 3 to 5 times greater H<sub>2</sub>SO<sub>4</sub> to the continental surface than the  
64 pyrite oxidation originated H<sub>2</sub>SO<sub>4</sub> (Lerman et al., 2007). Therefore, increasing acid  
65 precipitation due to stronger human activities nowadays could make this mechanism  
66 more prominently.

67 The role of acid precipitation on the chemical weathering and CO<sub>2</sub> consumption  
68 has been investigated in some river catchments (Amiotte-Suchet et al., 1995; Probst et  
69 al., 2000; Vries et al., 2003; Lerman et al., 2007; Xu and Liu, 2010). It has been  
70 documented that silicate rocks were more easily disturbed by acid precipitation during  
71 their weathering and soil leaching processes, because of their low buffering capacity  
72 (Reuss et al., 1987; Amiotte-Suchet et al., 1995). According to Amiotte-Suchet et al.  
73 (1995), especially where crystalline rocks outcrop, the disturbance can be very high  
74 and can induce a decrease of CO<sub>2</sub> consumption by weathering at least 73% in the  
75 Strengbach catchment (Vosges Mountains, France). This highlights the importance of  
76 exploring anthropogenic impact on chemical weathering and CO<sub>2</sub> consumption under



77 different background (e.g. lithology, climate, human activity intensity, and basin  
78 scale) for better constraining and estimation of acid precipitation effect on rock  
79 weathering. Asia, especially East Asia, is one of the world's major sulfur emissions  
80 areas. However, the effect of acid precipitation on silicate weathering and associated  
81 CO<sub>2</sub> consumption was not well evaluated in this area, especially lack of quantitative  
82 studies.

83 Southeast coastal region of China is the most highly developed and  
84 populated area in China, dominated by Mesozoic magmatic rocks (mainly granite and  
85 volcanic rocks) in lithology. Meanwhile, it is also seriously impacted by acid rain,  
86 with a volume-weighted mean value of pH lower than 4.5 for many years (Wang et al.,  
87 2000; Larssen and Carmichael, 2000; Zhao, 2004; Han et al., 2006; Larssen et al.,  
88 2006; Zhang et al., 2007a; Huang et al., 2008; Xu et al., 2011). Therefore, it is an  
89 ideal area for evaluating silicate weathering and the effect of acid rain. In this study,  
90 the chemical and carbon isotope composition of rivers in this area were first  
91 systematically investigated, in order to: (i) decipher the different sources of solutes  
92 and to quantify their contributions to the dissolved loads; (ii) calculate silicate  
93 weathering and associated CO<sub>2</sub> consumption rates; (iii) evaluate the effects of acid  
94 deposition on rock weathering and CO<sub>2</sub> consumption flux.

## 95 **2. Natural setting of study area**

96 Southeast coastal region of China, where the landscape is dominated by  
97 mountainous and hilly terrain, has rugged coastlines and develop numerous small and  
98 medium river system. Rivers in this region flow eastward or southward and finally



99 inject into the East China Sea or the South China Sea (Fig. 1), and they are  
100 collectively named as ‘Southeast Coastal Rivers’ (SECRs). Large rivers are listed here  
101 from north to south, they are: Qiantang, Cao’e, Ling, and Ou in Zhejiang province;  
102 Jiaoxi, Huotong, Ao, Min, Jin, and Jiulong in Fujian province; Han and Rong in  
103 Guangdong province.

104 The Southeast Coastal Rivers Basin (SECRB) belongs to the warm and humid  
105 subtropical oceanic monsoon climate. The average annual temperature and  
106 precipitation are 17-21°C and 1400-2000 mm, respectively. The precipitation mainly  
107 happens during May to September, and the minimum and maximum temperature  
108 often occurs in January and July. This area is one of the most developed areas in  
109 China, with a population more than 190 million (mean density of ~470  
110 individuals/km<sup>2</sup>), but the population mainly concentrated in the coastal urban areas.  
111 The vegetation coverage of these river basins is more than 60%, mainly subtropical  
112 evergreen-deciduous broadleaf forest and mostly distributing in mountains area.  
113 Cultivated land, and industries and cities are mainly located in the plain areas and  
114 lower reach of these rivers.

115 Geologically, three regional-scale fault zones are distributed across the SECRB  
116 region (Fig. 1). They are the sub-EW-trending Shaoxing-Jiangshan fault zone, the  
117 NE-trending Zhenghe-Dapu fault zone, and the NE-trending Changle-Nanao fault  
118 zone (Shu et al., 2009). These fault zones dominate the direction of the mountains  
119 ridgelines and drainages, as well as the formation of the basins and bay. The Zhenghe-  
120 Dapu fault zone is a boundary line of Caledonian uplift belt and Hercynian-Indosinian



121 depression zone. Mesozoic magmatic rocks are widespread in the southeast coastal  
122 region with a total outcrop area at about 240,000 km<sup>2</sup>. Over 90% of the Mesozoic  
123 magmatic rocks are granitoids (granites and rhyolites) and their volcanic counterpart  
124 with minor existence of basalts (Zhou et al., 2000, 2006; Bai et al., 2014). These crust-  
125 derived granitic rocks are mainly formed in the Yanshanian stage, and may have been  
126 related to multiple collision events between Cathaysia and Yangtze blocks. Among the  
127 major river basins, the proportions of magmatic rocks outcrop are about 36% in  
128 Qiantang river basin, above 80% in Ou, Jiaoxi and Jin river basins, and around 60% in  
129 Min, Jiulong, Han and Rong river basins (Shi, 2014). The overlying Quaternary  
130 sediment in this area is composed of brown-yellow siltstones but is rarely developed.  
131 The oldest basement complex is composed of metamorphic rocks of greenschist and  
132 amphibolite facies. Sedimentary rocks categories into two types, one is mainly  
133 composed by red clastic rocks which cover more than 40,000 km<sup>2</sup> in the study area;  
134 the other occurs as interlayers within volcanic formations, including varicolored  
135 mudstones and sandstones. They are mainly distributed on the west of Zhenghe-Dapu  
136 fault zone (FJBGRM, 1985; ZJBGMR, 1989; Shu et al., 2009).

### 137 **3. Sampling and analytical method**

138 Water samples were collected during the high-flow season of 2010 (sample  
139 number and locations are shown in Fig. 1). 2-L water samples were collected in the  
140 middle channel of the river from bridges or ferries, or directly from the center of some  
141 shallow streams in the source area. The lower reaches sampling sites were selected  
142 distant away from the estuary to avoid the influence of seawater. Temperature (T), pH



143 and electrical conductivity (EC) were measured in the field with a portable EC/pH  
144 meter (YSI-6920, USA). All of the water samples for chemical analysis were filtered  
145 in field through 0.22  $\mu\text{m}$  Millipore membrane filter, and the first portion of the  
146 filtration was discarded to wash the membrane and filter. One portion filtrate were  
147 stored directly in HDPE bottles for anion analysis and another were acidified to pH  
148  $<2$  with 6M double sub-boiling distilled  $\text{HNO}_3$  for cation analysis. All containers were  
149 previously washed with high-purity HCl and rinsed with Milli-Q 18.2  $\text{M}\Omega$  water.

150 Alkalinity was titrated with 0.005M HCl within 12 h after sampling. Cations  
151 ( $\text{Na}^+$ ,  $\text{K}^+$ ,  $\text{Ca}^{2+}$  and  $\text{Mg}^{2+}$ ) were determined using Inductively Coupled Plasma Atomic  
152 Emission Spectrometer (ICP-AES) (IRIS Intrepid II XSP, USA). Anions ( $\text{Cl}^-$ ,  $\text{F}^-$ ,  
153  $\text{NO}_3^-$  and  $\text{SO}_4^{2-}$ ) were analyzed by ionic chromatography (IC) (Dionex Corporation,  
154 USA). Dissolved silica was determined by spectrophotometry using the molybdate  
155 blue method. Reagent and procedural blanks were measured in parallel to the sample  
156 treatment, and calibration curve was evaluated by quality control standards before,  
157 during and after the analyses of each batch of samples. Measurement reproducibility  
158 was determined by duplicated sample and standards, which showed  $\pm 3\%$  precision for  
159 the cations and  $\pm 5\%$  for the anions.

160 River water samples for carbon isotopic ratio ( $\delta^{13}\text{C}$ ) of dissolved inorganic  
161 carbon (DIC) measurements were collected in 150 ml glass bottles with air-tight caps  
162 and preserved with  $\text{HgCl}_2$  to prevent biological activity. The samples were kept  
163 refrigerated until analysis. For the  $\delta^{13}\text{C}$  measurements, the filtered samples were  
164 injected into glass bottles with phosphoric acid. The  $\text{CO}_2$  was then extracted and



165 cryogenically purified using a high vacuum line.  $\delta^{13}\text{C}$  isotopic ratios were analyzed on  
166 Finnigen MAT-252 stable isotope mass spectrometer at the State Key Laboratory of  
167 Environmental Geochemistry, Chinese Academy of Sciences. The results are  
168 expressed with reference to VPDB, as follows:

$$169 \quad \delta^{13}\text{C} = \left[ \left( \frac{{}^{13}\text{C}/{}^{12}\text{C}}{\text{sample}} / \left( \frac{{}^{13}\text{C}/{}^{12}\text{C}}{\text{standard}} \right) - 1 \right) \times 1000 \right] \quad (1)$$

170 The  $\delta^{13}\text{C}$  measurement has an overall precision of 0.1‰. A number of duplicate  
171 samples were measured and the results show that the differences were less than the  
172 range of measurement accuracy.

#### 173 4. Results

174 The major parameter and ion concentrations of samples are given in Table 1. The  
175 pH values of water samples ranged from 6.50 to 8.24, with an average of 7.23. Total  
176 dissolved solids (TDS) of water samples varied from 35.3 to 205  $\text{mg l}^{-1}$ , with an  
177 average of 75.2  $\text{mg l}^{-1}$ . Comparing with the major rivers in China, the average TDS  
178 was significantly lower than Changjiang (224  $\text{mg l}^{-1}$ , Chetelat et al., 2008), Huanghe  
179 (557  $\text{mg l}^{-1}$ , Fan et al., 2014) and Zhujiang (190  $\text{mg l}^{-1}$ , Zhang et al., 2007b).  
180 However, the average TDS was comparable to the rivers draining silicate rock  
181 dominated areas, e.g. the upper Ganjiang (63  $\text{mg l}^{-1}$ , Ji and Jiang, 2012), the Amur (70  
182  $\text{mg l}^{-1}$ , Moon et al., 2009), Xishui (101  $\text{mg l}^{-1}$ , Wu et al., 2013), and north Han river in  
183 South Korea (75.5  $\text{mg l}^{-1}$ , Ryu et al., 2008). Among the major rivers in the SECRB,  
184 the Qiantang river had the highest TDS value (averaging at 121  $\text{mg l}^{-1}$ ), and the Ou  
185 river had the lowest TDS value (averaging at 48.8  $\text{mg l}^{-1}$ ).

186 Major ion compositions are shown in the cation and anion ternary diagrams (Fig.



187 2a and b). In comparison with rivers (e.g. the Wujiang and Xijiang) draining  
188 carbonate rocks dominated area (Han and Liu, 2004; Xu and Liu, 2010), these rivers  
189 in the SECRB have distinctly higher proportions of  $\text{Na}^+$ ,  $\text{K}^+$ , and dissolved  $\text{SiO}_2$ . As  
190 shown in the Fig. 2, most samples have high  $\text{Na}^+$  and  $\text{K}^+$  proportions, with an average  
191 higher than 50% (in  $\mu\text{mol l}^{-1}$ ) of the total cations, except for samples from the  
192 Qiantang river. The concentrations of  $\text{Na}^+$  and  $\text{K}^+$  range from 43.5 to 555  $\mu\text{mol l}^{-1}$  and  
193 42.9 to 233  $\mu\text{mol l}^{-1}$ , with average values of 152 and 98  $\mu\text{mol l}^{-1}$ , respectively. The  
194 concentrations of dissolved  $\text{SiO}_2$  range from 98.5 to 370  $\mu\text{mol l}^{-1}$ , with an average of  
195 212  $\mu\text{mol l}^{-1}$ .  $\text{Ca}^{2+}$  and  $\text{Mg}^{2+}$  account for about 38% and 11.6% of the total cation  
196 concentrations.  $\text{HCO}_3^-$  is the dominant anion with concentrations ranging from 139 to  
197 1822  $\mu\text{mol l}^{-1}$ . On average, it comprises 60.6% (36-84.6%) of total anions on a molar  
198 basis, followed by  $\text{SO}_4^{2-}$  (14.6%),  $\text{Cl}^-$  (13.1%) and  $\text{NO}_3^-$  (11.8%). The major ionic  
199 compositions indicate that water chemistry of these rivers in the SECRB is controlled  
200 by silicate weathering. Meanwhile, it is also influenced by carbonate weathering,  
201 especially in the Qiantang river system.

202 The  $\delta^{13}\text{C}$  of dissolved inorganic carbon in the rivers of the SECRB are given in  
203 Table 1. The  $\delta^{13}\text{C}$  of the water samples show a wide range, from -11.0‰ to -24.3‰  
204 (average -19.4‰), and with majority falling between -15 of -23‰. The values are  
205 similar to most rivers draining Deccan Traps (Das et al., 2005).

## 206 5. Discussion

207 The dissolved solids in river water are commonly from atmospheric and  
208 anthropogenic inputs and weathering of rocks within the drainage basin. It is



209 necessary to quantify the contribution of different sources to the dissolved loads  
210 before deriving chemical weathering rates and associated CO<sub>2</sub> consumption.

### 211 *5.1 Atmospheric and anthropogenic inputs*

212 To evaluate atmospheric inputs to river waters, chloride is the most common  
213 used reference. Generally, water samples that have the lowest Cl<sup>-</sup> concentrations are  
214 employed to correct the proportion of atmospheric inputs in a river system (Négrel et  
215 al., 1993; Gaillardet et al., 1997; Viers et al., 2001; Xu and Liu, 2007). In pristine  
216 areas, the concentration of Cl<sup>-</sup> in river water is assumed to be entirely derived from  
217 the atmosphere, provided that the contribution of evaporites is negligible. In the  
218 SECRB, the lowest Cl<sup>-</sup> concentration was mainly found in the headwater of each  
219 river. According to the geologic setting, no salt-bearing rocks was found in these  
220 headwater area (FJBGRM, 1985; ZJBGMR, 1989). In addition, these areas are mainly  
221 mountainous and sparsely populated. Therefore, we assumed that the lowest Cl<sup>-</sup>  
222 concentration of samples from the headwater of each major river came entirely from  
223 atmosphere.

224 The proportion of atmosphere-derived ions in the river waters can then be  
225 calculated by using the element/Cl ratios of the rain. Chemical compositions of rain in  
226 the studied area have been reported at different sites, including Hangzhou, Jinhua,  
227 Nanping, Fuzhou and Xiamen (Zhao, 2004; Zhang et al., 2007a; Huang et al., 2008;  
228 Cheng et al., 2011; Xu et al., 2011) (Fig. 1). The volume-weighted mean  
229 concentration of ions and Cl-normalized molar ratios are compiled in Table 2.  
230 According to this procedure, 6.6-23.4% (averaging 14.4%) of total dissolved cations



231 in the major rivers of the SECRB originated from rain. Among the anions,  $\text{SO}_4^{2-}$  and  
232  $\text{NO}_3^-$  in the rivers are mainly from the atmospheric input, averaging at 74.7% for  
233  $\text{SO}_4^{2-}$  and 68.6% for  $\text{NO}_3^-$ , respectively.

234 As the most developed and populated areas in China, the chemistry of rivers in  
235 the SECRB could be significantly impacted by anthropogenic inputs.  $\text{Cl}^-$ ,  $\text{NO}_3^-$  and  
236  $\text{SO}_4^{2-}$  are commonly associated with anthropogenic sources and have been used as  
237 tracers of anthropogenic inputs in watershed. High concentrations of  $\text{Cl}^-$ ,  $\text{NO}_3^-$  and  
238  $\text{SO}_4^{2-}$  can be found at the lower reaches of rivers in the SECRB, and an obvious  
239 increase after flowing through plain areas and city. This tendency indicates that river  
240 water chemistry is affected by anthropogenic inputs while passing through the  
241 catchments. After correcting for the atmospheric contribution to river waters, the  
242 following assumption is needed to quantitatively estimate the contributions of  
243 anthropogenic inputs. That is,  $\text{Cl}^-$  originates from only atmospheric and anthropogenic  
244 inputs, the excess of atmospheric  $\text{Cl}^-$  is regarded to present anthropogenic inputs and  
245 balanced by Na.

#### 246 *5.2 Chemical weathering inputs*

247 Water samples were displayed on a plot of Na-normalized molar ratios (Fig. 3).  
248 The values of the world's large rivers (Gaillardet et al. 1999) are also shown for  
249 comparison in the figure. A best correlations between elemental ratios were observed  
250 for  $\text{Ca}^{2+}/\text{Na}^+$  vs.  $\text{Mg}^{2+}/\text{Na}^+$  ( $R^2 = 0.95$ ,  $n = 120$ ) and  $\text{Ca}^{2+}/\text{Na}^+$  vs.  $\text{HCO}_3^-/\text{Na}^+$  ( $R^2 =$   
251  $0.98$ ,  $n = 120$ ). The samples cluster on a mixing line mainly between silicate and  
252 carbonate end members, closer to the silicate end-member, and with little evaporite



253 contribution. This corresponds with the distribution of rock types in the SECRB. In  
254 addition, all water samples have equivalent ratios of  $(\text{Na}^+ + \text{K}^+)/\text{Cl}^-$  larger than one,  
255 indicating silicate weathering as the source of  $\text{Na}^+$  and  $\text{K}^+$  rather than chloride  
256 evaporites dissolution.

257 The geochemical characteristics of the silicate and carbonate end-members can  
258 be deduced from the correlations between elemental ratios and referred to literature  
259 data for catchments with well-constrained lithology. After correction for atmospheric  
260 inputs, the  $\text{Ca}^{2+}/\text{Na}^+$ ,  $\text{Mg}^{2+}/\text{Na}^+$  and  $\text{HCO}_3^-/\text{Na}^+$  of the river samples ranged from 0.31  
261 to 30, 0.16 to 6.7, and 1.1 to 64.2, respectively. According to the geological setting  
262 (Fig. 1), there are some small rivers draining purely silicate areas in the SECRs  
263 drainage basins. Based on the elemental ratios of these rivers, we assigned the silicate  
264 end-member for this study as  $\text{Ca}^{2+}/\text{Na}^+ = 0.41 \pm 0.10$ ,  $\text{Mg}^{2+}/\text{Na}^+ = 0.20 \pm 0.03$  and  $\text{HCO}_3^-$   
265  $/\text{Na}^+ = 1.7 \pm 0.6$ . The ratio of  $(\text{Ca}^{2+} + \text{Mg}^{2+})/\text{Na}^+$  for silicate end-member was 0.61, which  
266 is close to the silicate end-member of world rivers ( $(\text{Ca}^{2+} + \text{Mg}^{2+})/\text{Na}^+ = 0.59 \pm 0.17$ ,  
267 Gaillardet et al., 1999). Moreover, several previous researches have documented the  
268 chemical composition of rivers, such as the Amur and the Songhuajiang in North  
269 China, the Xishui in the lower reaches of the Changjiang, and major rivers in South  
270 Korea (Moon et al., 2009; Liu et al., 2013; Wu et al., 2013; Ryu et al., 2008; Shin et  
271 al., 2011). These river basins has similar geological setting with the study area, we  
272 could further validate the composition of silicate end-member with their results.  
273  $\text{Ca}^{2+}/\text{Na}^+$  and  $\text{Mg}^{2+}/\text{Na}^+$  ratios of silicate end-member were reported for the Amur  
274 (0.36 and 0.22), the Songhuajiang (0.44±0.23 and 0.16), the Xishui (0.6±0.4 and



275 0.32±0.18), the Han (0.55 and 0.21) and six major rivers in South Korea (0.48 and  
276 0.20) in the studies above, well bracketing our estimation for silicate end-member.

277 Whereas, some samples show high concentrations of  $\text{Ca}^{2+}$ ,  $\text{Mg}^{2+}$  and  $\text{HCO}_3^-$ ,  
278 indicating the contribution of carbonate weathering. The samples collected in the  
279 upper reaches (Sample 12 and 13) in the Qiantang river fall close to the carbonate  
280 end-member documented for world large rivers (Gaillardet et al., 1999). In the present  
281 study,  $\text{Ca}^{2+}/\text{Na}^+$  ratio of 0.41±0.10 and  $\text{Mg}^{2+}/\text{Na}^+$  ratio of 0.20±0.03 for silicate end-  
282 member are used to calculate the contribution of  $\text{Ca}^{2+}$  and  $\text{Mg}^{2+}$  from silicate  
283 weathering. Finally, residual  $\text{Ca}^{2+}$  and  $\text{Mg}^{2+}$  are apportioned to carbonate weathering.

### 284 5.3 Chemical weathering rate in the SECRBs

285 Based on the above assumption, a forward model is employed to quantify the  
286 relative contribution of the different sources to the rivers of the SECRB in this study.  
287 (e.g. Galy and France-Lanord, 1999; Moon et al., 2007; Xu and Liu, 2007; 2010; Liu  
288 et al., 2013). The calculated contributions of different reservoir to the total cationic  
289 loads for large rivers and their major tributaries in the SECRB are presented in Fig. 4.  
290 On average, the dissolved cationic loads of the rivers in the study area originate  
291 dominantly from silicate weathering, which accounts for 38.3% (10.7-74.0%) of the  
292 total cationic loads in molar unit. Carbonate weathering and anthropogenic inputs  
293 account for 29.4% (3.9-62.0%) and 17.8% (0-55.2%), respectively. Contributions  
294 from silicate weathering are high in the Ou (55.7%), Huotong (55%), Ao (48%) and  
295 Min (48.4%) river catchments, which dominated by granitic and volcanic bedrocks. In  
296 contrast, high contribution from carbonate weathering is observed in the Qiantang



297 (56.6%) and Jiulong (38.5%) river catchments. The results manifest the lithology  
298 control on river solutes of drainage basin.

299 The chemical weathering rate of rocks is estimated by the mass budget, basin  
300 area and annual discharge, expressed in  $\text{ton km}^{-2} \text{ a}^{-1}$ . The silicate weathering rate  
301 (SWR) is calculated using major cationic concentrations from silicate weathering and  
302 assuming that all dissolved  $\text{SiO}_2$  is derived from silicate weathering (Xu and Liu,  
303 2010), as the equation below:

$$304 \quad \text{SWR} = ([\text{Na}]_{\text{sil}} + [\text{K}]_{\text{sil}} + [\text{Ca}]_{\text{sil}} + [\text{Mg}]_{\text{sil}} + [\text{SiO}_2]_{\text{riv}}) \times \text{discharge/area} \quad (2)$$

305 The assumption about Si could lead to overestimation of the silicate weathering  
306 rate, as part of silica may come from dissolution of biogenic sources rather than the  
307 weathering of silicate minerals (Millot et al., 2003; Shin et al., 2011). Thus, the  
308 cationic silicate weathering rates ( $\text{Cat}_{\text{sil}}$ ) were also calculated.

309 The carbonate weathering rate (CWR) is calculated based on the sum of  $\text{Ca}^{2+}$ ,  
310  $\text{Mg}^{2+}$  and  $\text{HCO}_3^-$  from carbonate weathering, with half of the  $\text{HCO}_3^-$  coming from  
311 carbonate weathering being derived from the atmosphere  $\text{CO}_2$ , as the equation below:

$$312 \quad \text{CWR} = ([\text{Ca}]_{\text{carb}} + [\text{Mg}]_{\text{carb}} + 1/2[\text{HCO}_3]_{\text{carb}}) \times \text{discharge/area} \quad (3)$$

313 The chemical weathering rates and fluxes are calculated for major rivers and  
314 their main tributaries in the SECRB, and the results are shown in Table 3. Silicate and  
315 carbonate weathering fluxes of these rivers (SWF and CWF) range from  $0.02 \times 10^6 \text{ t a}^{-1}$   
316 <sup>1</sup> to  $1.29 \times 10^6 \text{ t a}^{-1}$ , and from  $0.002 \times 10^6 \text{ t a}^{-1}$  to  $1.33 \times 10^6 \text{ t a}^{-1}$ , respectively. Among the  
317 rivers, Min river has the highest silicate weathering flux, and Qiantang river has the  
318 highest carbonate weathering flux. On the whole SECRB scale,  $5.23 \times 10^6 \text{ t a}^{-1}$  and



319  $4.90 \times 10^6 \text{ t a}^{-1}$  of dissolved solids originating from silicate and carbonate weathering,  
320 respectively, are transported into the East and South China Sea by rivers in this  
321 region. Comparing with three largest three river basins (Changjiang, Huanghe and  
322 Xijiang) in China, the flux of silicate weathering calculated for the SECRB is lower  
323 than Changjiang ( $9.5 \times 10^6 \text{ t a}^{-1}$ , Gaillardet et al. 1999), but higher than Huanghe  
324 ( $1.52 \times 10^6 \text{ t a}^{-1}$ , Fan et al., 2014) and Xijiang ( $2.62 \times 10^6 \text{ t a}^{-1}$ , Xu and Liu, 2010).

325 The silicate and carbonate chemical weathering rates for these river watersheds  
326 were  $10.0\text{-}29.6 \text{ t km}^{-2} \text{ a}^{-1}$  and  $1.0\text{-}54.1 \text{ t km}^{-2} \text{ a}^{-1}$ , respectively. The total rock  
327 weathering rate (TWR) for the whole SECRB is  $35.3 \text{ ton km}^{-2} \text{ a}^{-1}$ , higher than the  
328 world average ( $24 \text{ ton km}^{-2} \text{ a}^{-1}$ , Gaillardet et al., 1999). The cationic silicate  
329 weathering rates ( $\text{Cat}_{\text{sil}}$ ) ranges from 2.4 to  $10.8 \text{ ton km}^{-2} \text{ a}^{-1}$  for the river watersheds  
330 in the SECRB, averaging at  $6.0 \text{ ton km}^{-2} \text{ a}^{-1}$ . Furthermore, a good linear correlation  
331 ( $R^2 = 0.85$ ,  $n = 28$ ) is observed between the  $\text{Cat}_{\text{sil}}$  and runoff (Fig. 5), indicating  
332 silicate weathering rates is controlled by the runoff as documented in previous  
333 researches (e.g., Bluth and Kump, 1994; Gaillardet et al., 1999; Millot et al., 2002;  
334 Oliva et al., 2003; Wu et al., 2013; Pepin et al., 2013).

#### 335 *5.4 CO<sub>2</sub> consumption and the role of sulfuric acid*

336 To calculate atmospheric CO<sub>2</sub> consumption by silicate weathering (CSW) and by  
337 carbonate weathering (CCW), a charge-balanced state between rock chemical  
338 weathering-derived alkalinity and cations was assumed (Roy et al., 1999).

$$339 \quad [\text{CO}_2]_{\text{CSW}} = [\text{HCO}_3]_{\text{CSW}} = [\text{Na}]_{\text{sil}} + [\text{K}]_{\text{sil}} + 2[\text{Ca}]_{\text{sil}} + 2[\text{Mg}]_{\text{sil}} \quad (4)$$

$$340 \quad [\text{CO}_2]_{\text{CCW}} = [\text{HCO}_3]_{\text{CCW}} = [\text{Ca}]_{\text{carb}} + [\text{Mg}]_{\text{carb}} \quad (5)$$



341 The calculated CO<sub>2</sub> consumption rates by chemical weathering for each river in  
342 SECRB are shown in Table 3. CO<sub>2</sub> consumption rates by carbonate and silicate  
343 weathering are from 11.6 to 550×10<sup>3</sup> mol km<sup>-2</sup> a<sup>-1</sup> (averaging at 166×10<sup>3</sup> mol km<sup>-2</sup> a<sup>-1</sup>)  
344 and from 67.1 to 417×10<sup>3</sup> mol km<sup>-2</sup> a<sup>-1</sup> (averaging at 214×10<sup>3</sup> mol km<sup>-2</sup> a<sup>-1</sup>) for major  
345 river catchments in the SECRB. The regional fluxes of CO<sub>2</sub> consumption by silicate  
346 and carbonate weathering is about 63.6×10<sup>9</sup> mol a<sup>-1</sup> (0.76×10<sup>12</sup> g C a<sup>-1</sup>) and 50.4×10<sup>9</sup>  
347 mol a<sup>-1</sup> (0.60×10<sup>12</sup> g C a<sup>-1</sup>) in the SECRB.

348 However, in addition to CO<sub>2</sub>, H<sub>2</sub>SO<sub>4</sub> is well documented as a significant proton  
349 provider in rock weathering process (Galy and France-Lanord, 1999; Karim and  
350 Veizer, 2000; Yoshimura et al., 2001; Han and Liu, 2004; Spence and Telmer, 2005;  
351 Lerman and Wu, 2006; Xu and Liu 2007; 2010). Sulfuric acid can be generated by  
352 natural oxidation of pyrite and anthropogenic emissions of SO<sub>2</sub> from coal combustion  
353 and subsequently dissolve carbonate and silicate minerals. The consumption of CO<sub>2</sub>  
354 by rock weathering would be overestimated if H<sub>2</sub>SO<sub>4</sub> induced rock weathering is  
355 ignored (Spence and Telmer, 2005; Xu and Liu, 2010; Shin et al., 2011). Thus, the  
356 role of sulfuric acid on the chemical weathering is crucial for an accurate estimation  
357 of CO<sub>2</sub> consumption by rock weathering.

358 Rapid economic growth and increased energy demand have result in severe air  
359 pollution problems in China, indicated by the high levels of mineral acids  
360 (predominately sulfuric) observed in precipitation (Lassen and Carmichael, 2000; Pan  
361 et al., 2013; Liu et al., 2016). The national SO<sub>2</sub> emissions in 2010 reached to 30.8  
362 Tg/year (Lu et al., 2011). Previous study documented that fossil fuel combustion



363 accounts for the dominant sulfur deposition (~77%) in China (Liu et al., 2016).  
364 Southeast coastal region is the most severe acid rain polluted region in China, with a  
365 volume-weighted mean value of pH lower than 4.5 for many years (Wang et al., 2000;  
366 Larssen and Carmichael, 2000; Zhao, 2004; Larssen et al., 2006). Current sulfur and  
367 nitrogen depositions in the Southeast coastal region are still among the highest in  
368 China (Fang et al., 2013; Cui et al., 2014; Liu et al., 2016).

369 The involvement of protons originating from  $\text{H}_2\text{SO}_4$  in the river waters can be  
370 verified by the stoichiometry between cations and anions, shown in Fig. 6. In the  
371 rivers of the SECRB, the sum cations released by silicate and carbonate weathering  
372 were not balanced by either  $\text{HCO}_3^-$  or  $\text{SO}_4^{2-}$  (Fig. 6a), but were almost balanced by the  
373 sum of  $\text{HCO}_3^-$  and  $\text{SO}_4^{2-}$  (Fig. 6b). This implies that both  $\text{H}_2\text{CO}_3$  and  $\text{H}_2\text{SO}_4$  are the  
374 potential erosion agents in chemical weathering in the SECRB. The  $\delta^{13}\text{C}$  values of the  
375 water samples show a wide range, from -11.0‰ to -24.3‰, with an average of -  
376 19.4‰. The  $\delta^{13}\text{C}$  from soil is governed by the relative contribution from  $\text{C}_3$  and  $\text{C}_4$   
377 plant (Das et al., 2005). The studied areas have subtropical temperatures and  
378 humidity, and thus  $\text{C}_3$  processes are dominant. The  $\delta^{13}\text{C}$  of soil  $\text{CO}_2$  is derived  
379 primarily from  $\delta^{13}\text{C}$  of organic material which typically has a value of -24 to -34‰,  
380 with an average of -28‰ (Faure, 1986). According to previous studies, the average  
381 value for  $\text{C}_3$  trees and shrubs are from -24.4 to -30.5‰, and most of them are lower  
382 than -28‰ in south China (Chen et al., 2005; Xiang, 2006; Dou et al., 2013). After  
383 accounting for the isotopic effect from diffusion of  $\text{CO}_2$  from soil, the resulting  $\delta^{13}\text{C}$   
384 (from the terrestrial  $\text{C}_3$  plant process) should be ~ -25‰ (Cerling et al., 1991). This



385 mean DIC derived from silicate weathering by carbonic acid (100% from soil CO<sub>2</sub>)  
386 would yield a δ<sup>13</sup>C value of -25‰. Carbonate rocks are generally derived from marine  
387 system and, typically, have δ<sup>13</sup>C value close to zero. Thus, the theoretical δ<sup>13</sup>C value  
388 of DIC derived from carbonate weathering by carbonic acid (50% from soil CO<sub>2</sub> and  
389 50% from carbonate rocks) is -12.5‰. DIC derived from carbonate weathering by  
390 sulfuric acid are all from carbonate rocks, thus the δ<sup>13</sup>C of the DIC would be 0‰.  
391 Based on these conclusions, sources of riverine DIC from different end-members in  
392 the SECRB were plotted in Fig. 7. Most water samples drift away from the three  
393 endmember mixing area (carbonate and silicate weathering by carbonic acid and  
394 carbonate weathering by sulfuric acid) and towards the silicate weathering by H<sub>2</sub>SO<sub>4</sub>  
395 area, clearly illustrating the effect of sulfuric acid on silicate weathering.

396 Considering the H<sub>2</sub>SO<sub>4</sub> effect on chemical weathering, CO<sub>2</sub> consumption by  
397 silicate weathering can be determined from the equation below (Moon et al., 2007;  
398 Ryu et al., 2008; Shin et al., 2011):

$$399 \quad [\text{CO}_2]_{\text{SSW}} = [\text{Na}]_{\text{sil}} + [\text{K}]_{\text{sil}} + 2[\text{Ca}]_{\text{sil}} + 2[\text{Mg}]_{\text{sil}} - \gamma \times 2[\text{SO}_4]_{\text{atmos}} \quad (6)$$

400 Where  $\gamma$  is calculated by  $\text{cation}_{\text{sil}} / (\text{cation}_{\text{sil}} + \text{cation}_{\text{carb}})$ .

401 Based on the calculation in section 5.1, SO<sub>4</sub><sup>2-</sup> in river waters were mainly derived  
402 from atmospheric input. Assuming sulfate in rivers derived from atmospheric input  
403 (after correction for sea-salt contribution) are all from acid precipitation, CO<sub>2</sub>  
404 consumption rates by silicate weathering (SSW) are estimated between 31.8×10<sup>3</sup> mol  
405 km<sup>-2</sup> a<sup>-1</sup> and 363×10<sup>3</sup> mol km<sup>-2</sup> a<sup>-1</sup> for major river watersheds in the SECRB. For the  
406 whole SECRB, the actual CO<sub>2</sub> consumption rates by silicate is 167×10<sup>3</sup> mol km<sup>-2</sup> a<sup>-1</sup>



407 when the effect of  $\text{H}_2\text{SO}_4$  is considered. The flux of  $\text{CO}_2$  consumption is  
408 overestimated by  $15.8 \times 10^9 \text{ mol a}^{-1}$  ( $0.19 \times 10^{12} \text{ g C a}^{-1}$ ) due to the involvement of  
409 sulfuric acid from acid precipitation, accounting for approximately 24.9% of total  
410  $\text{CO}_2$  consumption flux by silicate weathering in the SECRB. It highlights the fact that  
411 the drawdown of atmospheric  $\text{CO}_2$  by silicate weathering can be significantly  
412 overestimated if acid deposition is ignored in short- and long-term perspectives. The  
413 result is important as it quantitatively shows that anthropogenic activities can  
414 significantly affect rock weathering and associated atmospheric  $\text{CO}_2$  consumption.  
415 The quantification of this effect needs to be well evaluated in Asian and global scale  
416 within the current and future human activity background.

## 417 **6. Conclusions**

418 River waters in the Southeast coastal region of China are characterized by high  
419 proportions of  $\text{Na}^+$ ,  $\text{K}^+$  and dissolved  $\text{SiO}_2$ , indicating water chemistry of the rivers in  
420 the SECRB is mainly controlled by silicate weathering. The dissolved cationic loads  
421 of the rivers in the study area originate dominantly from silicate weathering, which  
422 accounts for 38.3% (10.7-74.0%) of the total cationic loads. Carbonate weathering,  
423 atmospheric and anthropogenic inputs account for 29.4% (3.9-62.0%), 14.4% (6.6-  
424 23.4%) and 17.8% (0-55.2%), respectively. Meanwhile, more than 70% of  $\text{SO}_4^{2-}$  in  
425 the rivers derived from atmospheric input. The chemical weathering rate of silicates  
426 and carbonates for the whole SECRB are estimated to be approximately 18.2 and 17.1  
427  $\text{ton km}^{-2} \text{ a}^{-1}$ . About  $10.1 \times 10^6 \text{ t a}^{-1}$  of dissolved solids originating from rock weathering  
428 are transported into the East and South China Sea by these rivers. With the



429 assumption that all the protons involved in the weathering reaction are provided by  
430 carbonic acid, the CO<sub>2</sub> consumption rates by silicate and carbonate weathering are  
431 222 and 176×10<sup>3</sup> mol km<sup>-2</sup> a<sup>-1</sup>, respectively. However, both water chemistry and  
432 carbon isotope data provide evidence that sulfuric acid from precipitation serves as a  
433 significant agent during chemical weathering. Considering the effect of sulfuric acid,  
434 the CO<sub>2</sub> consumption rate by silicate weathering for the SECRB are 167×10<sup>3</sup> mol km<sup>-2</sup>  
435 a<sup>-1</sup>. Therefore, the CO<sub>2</sub> consumption flux would be overestimated by 15.8×10<sup>9</sup> mol a<sup>-1</sup>  
436 (0.19×10<sup>12</sup> g C a<sup>-1</sup>) in the SECRB if the effect of sulfuric acid is ignored. This work  
437 illustrates that anthropogenic disturbance by acid precipitation has profound impact  
438 on CO<sub>2</sub> sequestration by rock weathering.

439 **Acknowledgements.** This work was financially supported by Natural Science  
440 Foundation of China (Grant No. 41673020, 91747202, 41772380 and 41730857) and  
441 the "Strategic Priority Research Program" of the Chinese Academy of Sciences (Grant  
442 No. XDB15010405)

#### 443 **References:**

444 Amiotte-Suchet, P., Probst, A. Probst, J.-L., Influence of acid rain on CO<sub>2</sub>  
445 consumption by rock weathering: local and global scales. Water Air Soil Pollut.  
446 85, 1563-1568, 1995.

447 Amiotte-Suchet, P., Probst, J.-L. Ludwig, W., Worldwide distribution of continental  
448 rock lithology: implications for the atmospheric/soil CO<sub>2</sub> uptake by continental  
449 weathering and alkalinity river transport to the oceans. Global Biogeochem.  
450 Cycles 17, 1038-1052, 2003.



- 451 Bai, H., Song, L.S., Xia, W.P., Prospect analysis of hot dry rock (HDR) in Eastern part  
452 of Jiangxi province, *Coal Geol. China* 26, 41-44. (In Chinese), 2014.
- 453 Berner, R.A., Caldeira, K., The need for mass balance and feedback in the  
454 geochemical carbon cycle. *Geology* 25, 955-956, 1997.
- 455 Bluth, G.J.S., Kump, L.R., Lithological and climatological controls of river chemistry.  
456 *Geochim. Cosmochim. Acta* 58, 2341-2359, 1994.
- 457 Brantley, S.L., Lebedeva, M., Learning to read the chemistry of regolith to understand  
458 the Critical Zone. *Annual Review of Earth and Planetary Sciences*, 39: 387-416,  
459 2011.
- 460 Calmels, D., Gaillardet, J., Brenot, A., France-Lanord, C., Sustained sulfide oxidation  
461 by physical erosion processes in the Mackenzie River basin: climatic  
462 perspectives. *Geology* 35, 1003-1006, 2007.
- 463 Calmels, D., Galy, A., Hovius, N., Bickle, M., West, A.J., Chen, M.-C., Chapman, H.,  
464 Contribution of deep groundwater to the weathering budget in a rapidly eroding  
465 mountain belt, Taiwan. *Earth Planet. Sci. Lett.* 303, 48-58, 2011.
- 466 Cerling, T.E., Solomon, D.K., Quade, J., Bownman, J.R., On the isotopic composition  
467 of soil CO<sub>2</sub>. *Geochim. Cosmochim. Acta* 55, 3403–3405, 1991.
- 468 Chen, Q., Shen, C., Sun, Y., Peng, S., Yi, W., Li Z., Jiang, M., Spatial and temporal  
469 distribution of carbon isotopes in soil organic matter at the Dinghushan  
470 Biosphere Reserve, South China. *Plant and Soil*, 273: 115–128, 2005.
- 471 Cheng, Y., Liu, Y., Huo, M., Sun, Q., Wang, H., Chen, Z., Bai, Y., Chemical  
472 characteristics of precipitation at Nanping Mangdang Mountain in eastern China



- 473 during spring. *J. Environ. Sci.* 23, 1350-1358, 2011.
- 474 Chetelat, B., Liu, C., Zhao, Z., Wang, Q., Li, S., Li, J., Wang, B., Geochemistry of the  
475 dissolved load of the Changjiang Basin rivers: anthropogenic impacts and  
476 chemical weathering. *Geochim. Cosmochim. Acta* 72, 4254-4277, 2008.
- 477 Cui, J., Zhou, J., Peng, Y., He, Y., Yang, H., Mao, J., Atmospheric wet deposition of  
478 nitrogen and sulfur to a typical red soil agroecosystem in Southeast China  
479 during the ten-year monsoon seasons (2003-2012). *Atmos. Environ.* 82, 121-  
480 129, 2014.
- 481 Das, A., Krishnaswami, S., Sarin, M.M., Pande, K., Chemical weathering in the  
482 Krishna Basin and Western Ghats of the Deccan Traps, India: Rates of basalt  
483 weathering and their controls. *Geochim. Cosmochim. Acta* 69(8), 2067-2084,  
484 2005.
- 485 Dou, X., Deng, Q., Li, M., Wang, W., Zhang, Q., Cheng, X., Reforestation of *Pinus*  
486 *massoniana* alters soil organic carbon and nitrogen dynamics in eroded soil in  
487 south China. *Ecological Engineering* 52, 154-160, 2013.
- 488 Edmond, J.M., Palmer, M.R., Measures, C.I., Grant, B., Stallard, R.F., The fluvial  
489 geochemistry and denudation rate of the Guayana Shield in Venezuela,  
490 Colombia, and Brazil. *Geochim. Cosmochim. Acta* 59, 3301-3325, 1995.
- 491 Fan, B.L., Zhao, Z.Q., Tao, F.X., Liu, B.J., Tao, Z.H., Gao, S., He, M.Y.,  
492 Characteristics of carbonate, evaporite and silicate weathering in Huanghe River  
493 basin: A comparison among the upstream, midstream and downstream. *J. Asian*  
494 *Earth Sci.* 96, 17-26, 2014.



- 495 Fang, Y., Wang, X., Zhu, F., Wu, Z., Li, J., Zhong, L., Chen, D., Yoh, M., Three-  
496 decade changes in chemical composition of precipitation in Guangzhou city,  
497 southern China: has precipitation recovered from acidification following  
498 sulphur dioxide emission control? *Tellus B* 65, 1-15, 2013.
- 499 Faure, G., *Principles of Isotope Geology*. Wiley, Toronto, pp. 492-493, 1986.
- 500 FJBGMR: Fujian Bureau of Geology and Mineral Resources, *Regional Geology of*  
501 *Fujian Province*. Geol. Publ. House, Beijing, p. 671 (in Chinese with English  
502 abstract), 1985.
- 503 Gaillardet, J., Dupré, B., Allègre, C.J., Négrel, P., *Chemical and physical denudation*  
504 *in the Amazon River basin*. *Chem. Geol.* 142, 141-173, 1997.
- 505 Gaillardet, J., Dupré, B., Louvat, P., Allegre, C.J., *Global silicate weathering and CO<sub>2</sub>*  
506 *consumption rates deduced from the chemistry of large rivers*. *Chem. Geol.* 159,  
507 3-30, 1999.
- 508 Galy, A., France-Lanord, C., *Weathering processes in the Ganges-Brahmaputra basin*  
509 *and the riverine alkalinity budget*. *Chem. Geol.* 159, 31-60, 1999.
- 510 Gandois, L., Perrin, A.-S., Probst, A., *Impact of nitrogenous fertilizer-induced proton*  
511 *release on cultivated soils with contrasting carbonate contents: A column*  
512 *experiment*. *Geochim. Cosmochim. Acta* 75, 1185-1198, 2011.
- 513 Gislason, S.R., Arnorsson, S., Armannsson, H., *Chemical weathering of basalt in*  
514 *southwest Iceland: effects of runoff, age of rocks and vegetative/glacial cover*.  
515 *Am. J. Sci.* 296, 837-907, 1996.
- 516 Han, G., Liu, C.Q., *Water geochemistry controlled by carbonate dissolution: a study*



- 517 of the river waters draining karst-dominated terrain, Guizhou Province, China.  
518 Chem. Geol. 204, 1-21, 2004.
- 519 Han, Z.W., Ueda, H., Sakurai, T., Model study on acidifying wet deposition in East  
520 Asia during wintertime. Atmos. Environ. 40, 2360-2373, 2006.
- 521 Hartmann, J., Jansen, N., Dürr, H.H., Kempe, S., Köhler, P., Global CO<sub>2</sub> consumption  
522 by chemical weathering: what is the contribution of highly active weathering  
523 regions? Global Planet. Change 69, 185-194, 2009.
- 524 Huang, K., Zhuang, G., Xu, C., Wang Y., Tang A., The chemistry of the severe acidic  
525 precipitation in Shanghai, China. Atmos. Res. 89, 149-160, 2008.
- 526 Huh, Y.S., Chemical weathering and climate - a global experiment: a review. Geosci.  
527 J. 7, 277-288, 2003.
- 528 Ji, H., Jiang, Y., Carbon flux and C, S isotopic characteristics of river waters from a  
529 karstic and a granitic terrain in the Yangtze River system. J. Asian Earth Sci. 57,  
530 38-53, 2012.
- 531 Karim, A., Veizer, H.E., Weathering processes in the Indus River Basin: implication  
532 from riverine carbon, sulphur, oxygen and strontium isotopes. Chem. Geol. 170,  
533 153-177, 2000.
- 534 Kump, L.R., Brantley, S.L., Arthur, M.A., Chemical weathering, atmospheric CO<sub>2</sub> and  
535 climate. Ann. Rev. Earth Planet. Sci. 28, 611-667, 2000.
- 536 Larssen, T., Carmichael, G.R., Acid rain and acidification in China: the importance of  
537 base cation deposition. Environ. Poll. 110, 89-102, 2000.
- 538 Larssen, T., Lydersen, E., Tang, D., He, Y., Gao, J., Liu, H., Duan, L., Seip, H.M.,



- 539 Acid rain in China. *Environ. Sci. Technol.* 40, 418-425, 2006.
- 540 Lerman, A., Wu, L., CO<sub>2</sub> and sulfuric acid controls of weathering and river water  
541 composition. *J. Geochem. Explor.* 88, 427-430, 2006.
- 542 Lerman, A., Wu, L., Mackenzie, F.T., CO<sub>2</sub> and H<sub>2</sub>SO<sub>4</sub> consumption in weathering and  
543 material transport to the ocean, and their role in the global carbon balance. *Mar.*  
544 *Chem.* 106, 326-350, 2007.
- 545 Liu, B., Liu, C.-Q., Zhang, G., Zhao, Z.-Q., Li, S.-L., Hu, J., Ding, H., Lang, Y.-C.,  
546 Li, X.-D., Chemical weathering under mid- to cool temperate and monsoon-  
547 controlled climate: A study on water geochemistry of the Songhuajiang River  
548 system, northeast China. *Appl. Geochem.* 31, 265-278, 2013.
- 549 Liu, L., Zhang, X., Wang, S., Zhang, W., Lu, X., Bulk sulfur (S) deposition in China.  
550 *Atmos. Environ.*, 135, 41-49, 2016.
- 551 Lu, Z., Zhang, Q., Streets, D.G., Sulfur dioxide and primary carbonaceous aerosol  
552 emissions in China and India, 1996e2010. *Atmos. Chem. Phys.* 11, 9839-9864,  
553 2011.
- 554 Millot, R., Gaillardet, J., Dupré, B., Allègre, C.J., The global control of silicate  
555 weathering rates and the coupling with physical erosion: new insights from  
556 rivers of the Canadian Shield. *Earth Planet. Sci. Lett.* 196, 83-98, 2002.
- 557 Millot, R., Gaillardet, J., Dupré, B., Allègre, C.J., Northern latitude chemical  
558 weathering rates: clues from the Mackenzie River Basin, Canada. *Geochim.*  
559 *Cosmochim. Acta* 67, 1305-1329, 2003.
- 560 Moon, S., Chamberlain, C.P., Hilley, G.E., New estimates of silicate weathering rates



- 561 and their uncertainties in global rivers. *Geochim. Cosmochim. Acta* 134, 257-  
562 274, 2014.
- 563 Moon, S., Huh, Y., Qin, J., van Pho, N., Chemical weathering in the Hong (Red) River  
564 basin: Rates of silicate weathering and their controlling factors. *Geochim.*  
565 *Cosmochim. Acta* 71, 1411-1430, 2007.
- 566 Moon, S., Huh, Y., Zaitsev, A., Hydrochemistry of the Amur River: Weathering in a  
567 Northern Temperate Basin. *Aquat. Geochem.*, 15, 497-527, 2009.
- 568 Négrel, P., Allègre, C.J., Dupré, B., Lewin, E., Erosion sources determined by  
569 inversion of major and trace element ratios and strontium isotopic ratios in river  
570 water: the Congo Basin Case. *Earth Planet. Sci. Lett.* 120, 59-76, 1993.
- 571 Noh, H., Huh, Y., Qin, J., Ellis, A., Chemical weathering in the Three Rivers region of  
572 Eastern Tibet. *Geochim. Cosmochim. Acta* 73, 1857-1877, 2009.
- 573 Oliva, P., Viers, J., Dupré B., Chemical weathering in granitic environments. *Chem.*  
574 *Geol.* 202, 225-256, 2003.
- 575 Pan, Y., Wang, Y., Tang, G., Wu, D., Spatial distribution and temporal variations of  
576 atmospheric sulfur deposition in Northern China: insights into the potential  
577 acidification risks. *Atmos. Chem. Phys.* 13, 1675-1688, 2013.
- 578 Pepin, E., Guyot, J.L., Armijos, E., Bazan, H., Fraizy, P., Moquet, J.S., Noriega, L.,  
579 Lavado, W., Pombosa, R. Vauchel, P., Climatic control on eastern Andean  
580 denudation rates (Central Cordillera from Ecuador to Bolivia). *J. S. Am. Earth*  
581 *Sci.* 44, 85-93, 2013.
- 582 Perrin, A.-S., Probst, A., Probst, J.-L., Impact of nitrogenous fertilizers on carbonate



- 583 dissolution in small agricultural catchments: Implications for weathering CO<sub>2</sub>  
584 uptake at regional and global scales. *Geochim, Cosmochim. Acta* 72, 3105-  
585 3123, 2008.
- 586 Probst, A., Gh'mari, A.El., Aubert, D., Fritz, B., McNutt, R., Strontium as a tracer of  
587 weathering processes in a silicate catchment polluted by acid atmospheric  
588 inputs, Strengbach, France. *Chem. Geol.* 170, 203-219, 2000.
- 589 Raymo, M.E., Ruddiman, W.F., Tectonic forcing of late Cenozoic climate. *Nature* 359,  
590 117-122, 1992.
- 591 Reuss, J.O., Cosby, B.J., Wright, R.F., Chemical processes governing soil and water  
592 acidification. *Nature* 329, 27-32, 1987.
- 593 Roy, S., Gaillardet, J., Allègre, C.J., Geochemistry of dissolved and suspended loads  
594 of the Seine river, France: anthropogenic impact, carbonate and silicate  
595 weathering. *Geochim. Cosmochim. Acta* 63, 1277-1292, 1999.
- 596 Ryu, J.S., Lee, K.S., Chang, H.W., Shin, H.S., Chemical weathering of carbonates and  
597 silicates in the Han River basin, South Korea. *Chem. Geol.* 247, 66-80, 2008.
- 598 Semhi, K., Amiotte Suchet, P., Clauer, N., Probst, J.-L., Impact of nitrogen fertilizers  
599 on the natural weathering-erosion processes and fluvial transport in the Garonne  
600 basin. *Appl. Geochem.* 15 (6), 865-874, 2000.
- 601 Shi, C., Chemical characteristics and weathering of rivers in the Coast of Southeast  
602 China (PhD Thesis). Institute of Geology and Geophysics, Chinese academy of  
603 sciences, Beijing, China. Pp, 1-100 (in Chinese with English abstract), 2014.
- 604 Shin, W.-J., Ryu, J.-S., Park, Y., Lee, K.-S., Chemical weathering and associated CO<sub>2</sub>



- 605 consumption in six major river basins, South Korea. *Geomorphology* 129, 334-  
606 341, 2011.
- 607 Shu, L.S., Zhou, X.M., Deng, P., Wang, B., Jiang, S.Y., Yu, J.H., Zhao, X.X.,  
608 Mesozoic tectonic evolution of the Southeast China Block: New insights from  
609 basin analysis. *Journal of Asian Earth Sciences* 34(3), 376-391, 2009.
- 610 Spence, J., Telmer, K., The role of sulfur in chemical weathering and atmospheric  
611 CO<sub>2</sub> fluxes: Evidence from major ions,  $\delta^{13}\text{C}_{\text{DIC}}$ , and  $\delta^{34}\text{S}_{\text{SO}_4}$  in rivers of the  
612 Canadian Cordillera. *Geochim. Cosmochim. Acta* 69, 5441-5458, 2005.
- 613 U.S. Nat. Res. Council Comm., Basic Research Opportunities in Earth Science.  
614 Washington, DC: Nat. Acad. 154 pp., 2001.
- 615 Viers, J., Dupré, B., Braun, J.J., Freydier, R., Greenberg, S., Ngoupayou, J.N.,  
616 Nkamdjou, L.S., Evidence for non-conservative behavior of chlorine in humid  
617 tropical environments. *Aquat. Geochem.* 7, 127-154, 2001.
- 618 Vries, W.D., Reinds, G.J. Vel E., Intensive monitoring of forest ecosystems in Europe.  
619 2-Atmospheric deposition and its impacts on soil solution chemistry. *For. Ecol.*  
620 *Manage.* 174, 97-115, 2003.
- 621 Wang, T.J., Jin, L.S., Li, Z.K., Lam K.S., A modeling study on acid rain and  
622 recommended emission control strategies in China. *Atmos. Environ.* 34, 4467-  
623 4477, 2000.
- 624 West, A.J., Galy, A., Bickle, M., Tectonic and climatic controls on silicate weathering.  
625 *Earth Planet. Sci. Lett.* 235, 211-228, 2005.
- 626 Wu, W., Zheng, H., Yang, J., Luo, C., Zhou, B., Chemical weathering, atmospheric



- 627 CO<sub>2</sub> consumption, and the controlling factors in a subtropical metamorphic-  
628 hosted watershed. *Chem. Geol.* 356, 141-150, 2013.
- 629 Xiang, L., Study on Coupling between Water and Carbon of Artificial Forests  
630 Communities in Subtropical Southern China. Master Dissertation, Institute of  
631 Geographical Sciences and Natural Sources, Chinese Academy of Sciences,  
632 China (in Chinese), 2006.
- 633 Xu, H., Bi, X-H., Feng, Y-C., Lin, F-M., Jiao, L., Hong, S-M., Liu, W-G., Zhang, X.-  
634 Y., Chemical composition of precipitation and its sources in Hangzhou, China.  
635 *Environ. Monit. Assess.* 183:581-592, 2011.
- 636 Xu, Z., Liu, C.-Q., Chemical weathering in the upper reaches of Xijiang River  
637 draining the Yunnan-Guizhou Plateau, Southwest China. *Chem. Geol.* 239, 83-  
638 95, 2007.
- 639 Xu, Z., Liu, C.-Q., Water geochemistry of the Xijiang basin rivers, South China:  
640 Chemical weathering and CO<sub>2</sub> consumption. *Appl. Geochem.* 25, 1603-1614,  
641 2010.
- 642 Yoshimura, K., Nakao, S., Noto, M., Inokura, Y., Urata, K., Chen, M., Lin, P.W.,  
643 Geochemical and stable isotope studies on natural water in the Taroko Gorge  
644 karst area, Taiwan - chemical weathering of carbonate rocks by deep source  
645 CO<sub>2</sub> and sulfuric acid. *Chem. Geol.* 177, 415–430, 2001.
- 646 Zhang, M., Wang, S., Wu, F., Yuan, X., Zhang, Y., Chemical compositions of wet  
647 precipitation and anthropogenic influences at a developing urban site in  
648 southeastern China. *Atmos. Res.* 84, 311-322, 2007a.



- 649 Zhang, S.R., Lu, X. X., Higgitt, D. L., Chen, C.T.A., Sun, H.-G., Han, J.T., Water  
650 chemistry of the Zhujiang (Pearl River): Natural processes and anthropogenic  
651 influences. *J. Geophys. Res.* 112, F01011, 2007b.
- 652 Zhao, W., An analysis on the changing trend of acid rain and its causes in Fujian  
653 Province. *Fujian Geogr.* 19, 1-5 (in Chinese), 2004.
- 654 Zhou, X.M., Li, W.X., Origin of Late Mesozoic igneous rocks in Southeastern China:  
655 Implications for lithosphere subduction and underplating of mafic magmas.  
656 *Tectonophysics* 326(3-4), 269-287, 2000.
- 657 Zhou, X.M., Sun, T., Shen, W.Z., et al., Petrogenesis of Mesozoic granitoids and  
658 volcanic rocks in South China: A response to tectonic evolution. *Episodes* 29(1),  
659 26-33, 2006.
- 660 ZJBGMR: Zhejiang Bureau of Geology and Mineral Resources, Regional Geology of  
661 Zhejiang Province. Geol. Publ. House, Beijing, p. 617 (in Chinese with English  
662 abstract), 1989.



Table 1 Chemical and carbon isotopic compositions of river waters in the Southeast Coastal Rivers Basin (SECRB) of China.

Rivers	Sample number	Date (M/D/Y)	pH	T °C	EC $\mu\text{S cm}^{-1}$	Na <sup>+</sup> $\mu\text{M}$	K <sup>+</sup> $\mu\text{M}$	Mg <sup>2+</sup> $\mu\text{M}$	Ca <sup>2+</sup> $\mu\text{M}$	F <sup>-</sup> $\mu\text{M}$	Cl <sup>-</sup> $\mu\text{M}$	NO <sub>3</sub> <sup>-</sup> $\mu\text{M}$	SO <sub>4</sub> <sup>2-</sup> $\mu\text{M}$	HCO <sub>3</sub> <sup>-</sup> $\mu\text{M}$	SiO <sub>2</sub> $\mu\text{M}$	TZ+ $\mu\text{Eq}$	TZ- $\mu\text{Eq}$	NICB %	$\delta^{13}\text{C}$ ‰	TDS $\text{mg l}^{-1}$
Qiantang R.	1	07-8-10	7.42	28.78	190	347	197	106	473	12.0	303	62.6	147	1130	148	1703	1789	-5.0	-19.0	144
	2	07-9-10	7.60	23.84	146	87.5	204	80.9	496	11.7	75.2	124	121	907	156	1446	1348	6.7	-19.8	119
	3	07-9-10	7.37	27.83	308	555	233	208	698	41.8	312	223	437	1170	170	2601	2579	0.9	-17.8	204
	4	07-10-10	7.27	26.28	177	176	135	116	544	15.7	151	142	170	985	175	1632	1618	0.8	-19.3	135
	5	07-10-10	7.05	24.15	123	130	101	66.2	349	17.7	94.3	124	157	529	169	1061	1061	0.0	-18.7	91.2
	6	07-10-10	7.24	23.75	140	97.6	69.7	81.0	451	20.0	62.1	109	204	703	164	1231	1282	-4.2	-21.3	106.6
	7	07-11-10	7.40	23.23	107	92.5	70.5	68.3	327	14.9	74.9	104	147	486	156	954	960	-0.6	-21.0	82.2
	8	07-11-10	7.16	27.61	281	361	87.5	128	469	26.8	245	191	239	810	179	1642	1724	-5.0	-12.9	137.5
	9	07-11-10	7.02	26.48	140	275	120	60.7	319	36.2	199	150	180	437	236	1155	1146	0.8	-13.9	100.2
	10	07-12-10	7.05	24.24	99	205	114	58.3	285	14.6	191	114	132	305	278	1005	874	13.1	-20.9	85.4
	11	07-12-10	7.05	27.01	102	123	133	49.8	284	18.6	86.5	123	144	377	183	924	874	5.4	-19.2	79.4
	12	07-12-10	7.99	24.18	260	50.0	85.4	212	993	-	66.8	153	235	1822	172	2546	2512	1.4	-17.6	205.2
	13	07-12-10	7.86	24.59	231	43.5	88.4	189	859	-	55.1	97.6	169	1763	170	2228	2253	-1.1	-18.7	185.4
	14	07-12-10	7.69	22.66	131	44.1	81.0	113	458	-	19.1	95.2	107	920	143	1266	1248	1.4	-18.1	106.8
	15	07-12-10	7.65	24.48	106	61.1	98.3	87.9	335	-	37.2	68.3	112	663	164	1005	992	1.4	-18.6	87.3
	16	07-12-10	7.46	23.68	125	64.3	108	117	406	-	25.9	75.0	174	687	164	1218	1136	6.7	-20.0	98.8
	17	07-13-10	7.33	24.08	139	59.8	116	136	429	-	29.6	80.4	209	752	162	1305	1281	1.9	-20.8	108.1
	18	07-10-10	7.27	25.74	141	163	114	69.6	396	27.3	126	148	161	597	153	1209	1195	1.1	-21.0	101.0
Cao'e R.	19	07-16-10	7.17	22.27	108	212	86.3	69.4	183	5.1	151	148	114	384	216	803	912	-13.5	-21.2	79.1
	20	07-16-10	7.06	26.57	182	401	77.6	145	275	18.3	269	185	245	534	215	1318	1478	-12.2	-20.5	116.9
	21	07-16-10	7.14	27.26	171	333	91.3	164	362	18.1	224	194	207	658	225	1475	1490	-1.0	-20.9	123.3
	22	07-16-10	7.08	27.17	173	346	94.4	168	364	18.8	247	200	211	656	222	1506	1526	-1.3	-13.0	125.2
Ling R.	23	07-15-10	7.07	24.14	52	164	42.9	34.9	140	4.9	40.7	61.5	68.3	277	190	558	516	7.6	-12.8	52.1
	24	07-15-10	7.02	26.04	74	169	92.0	34.2	150	6.4	87.0	77.3	92.8	272	196	629	622	1.1	-20.8	59.5
	25	07-16-10	7.34	25.03	92	159	80.1	47.3	235	19.3	78.0	71.4	105	455	187	804	815	-1.4	-22.5	73.9
	26	07-16-10	7.40	26.75	113	216	77.8	57.1	249	20.2	133	90.0	115	494	196	905	946	-4.5	-12.7	82.8
	27	07-16-10	7.39	26	89	174	86.4	56.4	209	9.0	99.3	78.4	99.9	420	199	792	798	-0.8	-14.0	72.7
	28	07-15-10	6.79	22.33	75	159	82.7	44.1	143	-	107	61.8	83.4	306	144	616	641	-4.1	-21.1	56.5
	29	07-15-10	8.24	27.15	129	228	92.1	83.1	317	17.2	177	90.5	120	641	194	1120	1148	-2.5	-19.2	97.8
Ou R.	30	07-13-10	8.08	28.45	48	95.2	107	38.4	92.1	15.2	31.8	43.3	47.4	291	221	463	461	0.4	-21.7	50.6
	31	07-13-10	6.71	22.97	32	60.7	106	12.6	65.0	10.8	28.9	45.0	48.9	158	169	322	329	-2.2	-23.8	36.9
	32	07-13-10	7.18	27.59	73	107	127	36.2	175	4.3	57.1	111	92.0	283	210	655	634	3.2	-23.4	62.9
	33	07-13-10	6.94	24.2	44	76.9	112	20.0	99.1	10.9	27.9	63.1	58.6	249	184	427	457	-7.0	-22.5	47.5
	34	07-14-10	7.16	27.45	90	187	127	41.2	199.5	17.0	85.6	102	116	367	251	796	787	1.1	-22.4	76.5
	35	07-14-10	6.97	24.56	54	105	50.9	29.2	122	12.2	46.1	67.8	73.1	218	193	460	478	-4.1	-22.5	47.9
	36	07-14-10	6.82	21.12	31	76.4	133	12.7	74.5	7.7	20.7	36.8	49.1	192	162	383	348	9.3	-	39.5
	37	07-14-10	6.82	23.69	45	89.5	105	19.0	97.8	10.6	39.6	52.8	59.1	231	185	428	441	-3.0	-22.9	46.2
	38	07-15-10	6.92	24.69	37	100	89.3	21.1	49.7	1.7	36.9	45.5	52.7	153	202	331	341	-2.9	-	38.9
	39	07-15-10	6.90	23.86	35	92.2	92.0	19.8	61.4	1.9	43.9	47.9	55.5	139	193	347	342	1.4	-22.3	38.5
	40	07-15-10	7.09	25.56	47	117	112	25.7	83.4	8.0	52.4	63.1	57.4	232	193	447	462	-3.3	-22.5	48.1
	41	07-14-10	6.97	24.25	53	102	107	27.6	119	13.4	43.5	59.4	73.2	277	183	502	526	-4.9	-13.7	52.3



Feiyun R.	42	07-17-10	7.28	25.19	38	94.0	81.7	24.0	75.6	11.4	59.9	45.7	51.9	149	151	375	358	4.5	-	37.2
	43	07-17-10	7.08	25.61	46	101	79.9	33.9	93.4	4.6	66.2	55.1	52.8	223	151	435	450	-3.3	-23.7	43.5
Jiaoxi R.	44	07-17-10	7.52	26.92	47	116	81.5	25.2	92.0	4.1	73.3	80.3	25.0	226	151	432	430	0.5	-23.4	43.0
	45	07-17-10	7.45	27.46	61	152	90.2	34.2	119	-	136	59.8	53.5	238	184	548	542	1.2	-23.1	51.8
	46	07-18-10	6.90	27.66	53	127	88.1	33.4	94.4	7.0	123	93.1	30.4	209	177	471	486	-3.3	-14.4	47.4
Huotong R.	47	07-18-10	7.34	24	43	116	78.8	26.1	58.4	5.4	68.7	49.7	20.1	197	190	364	355	2.3	-22.8	39.6
Ao R.	48	07-19-10	7.24	31.44	124	294	121	102	209	24.3	204	73.6	52.0	717	370	1036	1100	-6.1	-19.4	105.4
	49	07-19-10	7.13	27.82	46	109	96.3	30.0	73.8	-	72.0	51.3	22.5	234	236	413	402	2.6	-	46.2
	50	07-18-10	6.98	28.65	53	140	88.4	40.8	100	3.0	82.9	58.6	20.9	294	233	511	477	6.6	-22.3	52.2
Min R.	51	07-27-10	7.11	28.4	42	116	92.0	40.5	119	18.0	43.9	35.5	26.0	382	182	526	513	2.4	-19.4	52.7
	52	07-27-10	7.17	30	51	102	97.9	41.7	107	4.6	29.4	45.3	35.0	350	221	496	495	0.2	-	53.3
	53	07-27-10	7.08	29.4	99	214	92.7	46.4	126	18.4	50.1	39.8	118	327	154	651	654	-0.4	-20.8	74.0
	54	07-27-10	7.06	29.1	44	107	99.6	28.1	114	16.4	18.7	36.4	44.3	305	265	491	449	8.5	-17.6	53.6
	55	07-27-10	7.42	29.4	57	139	93.7	49.8	113	3.1	67.1	56.3	26.6	384	236	558	561	-0.5	-16.4	58.6
	56	07-27-10	7.12	27.8	51	103	91.0	50.8	106	4.7	82.8	35.1	63.5	249	225	507	494	2.5	-	51.3
	57	07-27-10	7.08	27.5	40	125	45.0	36.8	107	12.1	43.6	44.5	29.3	288	211	457	435	5.0	-21.1	47.4
	58	07-27-10	6.99	27.2	52	121	98.0	42.4	115	16.7	87.1	36.6	70.9	277	228	535	542	-1.4	-11.4	55.3
	59	07-27-10	6.87	29	59	154	91.4	59.4	124	16.5	77.8	36.7	88.3	272	222	612	563	8.0	-20.3	57.2
	60	07-27-10	7.31	27.1	78	109	92.1	59.1	181	21.2	123	37.5	78.4	355	202	682	672	1.4	-18.7	63.1
	61	07-27-10	7.22	27.8	37	122	83.3	52.8	142	17.4	111	37.3	80.4	288	221	596	597	-0.2	-22.3	58.1
	62	07-27-10	7.16	28.1	58	104	83.3	59.3	163	24.0	34.6	34.5	118	294	214	632	599	5.2	-13.4	59.5
	63	07-27-10	7.26	28.3	87	139	86.1	60.9	191	14.8	48.0	93.0	109	347	226	729	707	3.0	-21.4	68.6
	64	07-27-10	7.00	28.8	87	127	93.1	58.7	195	6.6	59.8	81.1	60.9	480	232	729	743	-2.0	-11.0	74.0
	65	07-28-10	6.97	27.9	37	163	82.1	52.2	140	20.2	53.1	60.0	106	306	221	630	632	-0.2	-	61.9
	66	07-13-10	7.07	27.96	59	91.9	110	40.0	127	24.8	62.0	79.3	62.3	249	228	535	515	3.8	-	54.8
	67	07-28-10	7.12	29.7	38	108	93.4	45.9	133	12.4	48.3	34.0	56.6	368	220	560	564	-0.7	-	57.7
	68	07-27-10	7.03	29.9	62	128	96.7	57.6	148	23.3	81.6	36.8	74.1	374	203	635	641	-0.9	-12.4	61.7
	69	07-27-10	7.01	28.8	60	102	89.1	73.6	138	9.6	50.6	74.1	32.7	417	233	615	607	1.3	-21.0	62.3
	70	07-27-10	7.06	26.5	37	93.5	93.1	34.7	87.3	-	26.6	34.8	37.1	312	222	431	448	-3.9	-13.1	49.1
	71	07-27-10	7.09	26.5	25	62.6	92.7	27.0	61.5	4.7	21.5	18.6	43.4	191	154	332	318	4.2	-16.0	35.3
	72	07-28-10	7.07	30.1	39	76.3	87.9	35.1	87.6	7.4	43.1	36.6	35.5	266	175	409	416	-1.7	-19.4	43.5
	73	07-27-10	7.01	28.7	47	84.9	95.4	56.7	106	12.7	51.8	49.2	57.2	315	211	506	531	-4.8	-	53.8
	74	07-27-10	6.85	28.7	50	93.6	85.9	52.4	107	14.1	62.8	57.5	57.0	252	217	498	487	2.2	-19.9	50.9
	75	07-27-10	7.11	29.7	69	117	85.2	73.4	159	7.6	63.7	75.2	47.4	418	230	666	652	2.2	-22.2	65.0
	76	07-28-10	6.93	28.9	59	112	88.0	61.8	122	6.0	57.4	89.3	42.0	349	224	568	580	-2.2	-22.0	58.8
	77	07-21-10	7.76	32.4	51.2	163	85.5	52.8	151	20.2	55.3	70.3	78.6	372	175	656	655	0.3	-12.5	61.8
	78	07-28-10	7.29	26.8	106	129	75.3	84.0	321	24.0	56.2	41.0	166	599	202	1013	1028	-1.4	-16.3	90.3
	79	07-21-10	7.09	26.96	56	112	87.6	37.1	129	4.5	51.5	44.9	61.9	327	276	531	547	-2.9	-22.2	59.1
	80	07-21-10	7.64	33.37	83	114	96.2	60.6	151	16.7	53.0	40.6	102	371	242	633	670	-5.8	-12.8	66.2
	81	07-21-10	7.83	31.27	65	131	102	52.7	141	16.1	45.3	49.7	91.8	324	239	620	603	2.8	-13.4	61.8
	82	07-21-10	6.84	28.35	66	132	101	52.5	141	5.8	63.8	54.1	91.6	304	243	621	606	2.5	-22.7	61.5
	83	07-21-10	7.42	30.7	98	217	113	59.2	210	18.4	98.7	63.5	84.7	496	320	868	827	4.6	-18.9	84.5
	84	07-27-10	7.26	26.3	46	104	102	29.7	121	3.6	55.2	51.9	55.5	294	193	507	512	-0.9	-21.6	51.9
	85	07-27-10	7.07	25.4	30	73.3	99.2	19.6	78.8	-	22.9	40.0	49.2	203	170	369	365	1.3	-21.1	39.8
	86	07-27-10	7.50	27.3	45	102	102	26.5	114	2.4	35.1	39.7	57.2	260	217	484	449	7.3	-15.7	49.6
	87	07-27-10	7.47	26.9	51	141	100	43.6	109	7.9	79.7	42.4	57.7	311	217	547	548	-0.3	-20.1	55.6



	88	07-19-10	7.99	31.74	63	167	96.5	33.5	115	8.0	105	35.5	38.1	331	218	561	548	2.3	-13.5	55.9
	89	07-21-10	6.77	28.19	65	132	93.6	56.0	145	15.6	60.6	78.8	75.4	333	243	627	624	0.5	-22.6	63.3
Jin R.	90	07-27-10	7.36	25.8	128	126	94.8	88.9	406	22.9	51.4	39.4	229	595	208	1211	1143	5.6	-20.7	100
	91	07-27-10	7.40	26.9	123	143	103	82.7	347	21.0	83.5	203	182	463	226	1105	1115	-0.9	-21.3	98.4
	92	07-27-10	7.00	27.4	88	170	98.8	56.8	205	7.2	137	117	106	327	205	793	792	0.1	-22.5	71.8
	93	07-27-10	7.32	28.7	73	201	116	87.1	318	20.0	93.5	41.5	189	508	267	1128	1020	9.6	-21.7	95.3
Jiulong R.	94	07-30-10	6.50	23.47	29	72.3	92.4	22.8	59.8	12.4	25.1	27.0	50.0	189	213	330	341	-3.4	-18.1	40.1
	95	07-30-10	7.06	29.35	120	136	96.9	106	339	5.1	67.7	66.3	249	469	202	1124	1100	2.1	-20.8	94.2
	96	07-30-10	7.45	27.6	104	79.5	97.5	106	363	14.4	70.7	50.0	99.9	729	184	1116	1049	6.0	-18.9	93.7
	97	07-31-10	7.36	26.59	139	140	100	142	432	15.5	79.6	78.3	274	573	196	1388	1278	8.0	-19.7	108.8
	98	07-31-10	7.72	26.18	88	77.6	96.2	69.0	313	19.9	39.7	34.6	63.8	731	251	938	933	0.5	-18.4	89.4
	99	07-30-10	7.43	26.96	119	200	93.8	100.2	298	19.9	122	80.5	225	387	202	1091	1040	4.7	-20.5	89.5
	100	07-28-10	7.41	26.66	112	173	97.9	94.4	286	46.1	118	152	201	364	207	1033	1036	-0.3	-20.9	92.2
	101	07-29-10	7.16	29.35	82	151	110	55.4	178	4.9	71.2	170	53.2	385	305	727	732	-0.7	-21.2	76.1
	102	07-29-10	7.10	28.9	100	222	98.3	49.4	249	3.6	126	157	52.7	532	303	917	920	-0.3	-21.7	90.0
	103	07-28-10	7.20	31.15	138	339	111	81.2	277	9.2	280	285	88.6	515	317	1165	1256	-7.8	-19.0	112
	104	07-28-10	7.16	27.09	101	261	95.8	81.7	235	40.3	173	80.1	174	291	136	990	892	9.9	-24.3	75.4
Zhang R.	105	07-28-10	8.08	30.6	93	195	96.1	61.1	167	16.8	157	193	55.2	281	288	748	741	0.9	-21.5	73.8
Dongxi R.	106	07-28-10	7.20	30.9	78	263	99.0	41.5	115	14.5	238	65.3	30.0	283	309	675	646	4.4	-20.8	66.7
Huangang R.	107	07-28-10	7.40	30.5	99	253	85.6	53.0	154	7.7	190	63.5	56.4	460	278	754	827	-9.6	-20.0	77.4
Han R.	108	07-31-10	7.31	27.1	68	136	61.5	45.2	195	16.1	37.7	45.3	93.7	345	218	678	615	9.2	-21.9	62.0
	109	07-30-10	7.38	26.94	88	116	103	63.6	265	6.4	53.4	72.2	84.9	584	244	876	879	-0.4	-20.4	83.7
	110	07-30-10	6.66	25.55	71	114	96.2	47.6	168	8.0	56.9	54.6	143	230	203	642	628	2.2	-17.9	59.7
	111	07-30-10	6.66	27.76	83	135	104	63.8	203	8.6	54.5	74.9	173	302	336	774	777	-0.4	-20.6	78.7
	112	07-30-10	7.31	30.81	56	168	74.0	39.1	118	13.5	62.9	44.4	81.4	237	245	556	507	8.8	-21.4	54.6
	113	07-31-10	7.28	28.73	98	137	99.3	85.6	270	9.2	88.8	59.1	118	565	233	948	949	-0.1	-19.7	86.6
	114	07-31-10	7.27	31.42	123	193	105	98.2	319	20.7	120	102	157	570	229	1132	1107	2.2	-19.7	98.2
	115	07-30-10	7.43	29.89	85	115	97.5	65.5	244	6.5	46.5	58.6	103	511	251	832	822	1.1	-20.8	79.3
	116	07-31-10	7.61	30.98	99	123	104	85.9	264	5.6	58.8	90.9	108	588	98	926	952	-2.9	-20.0	79.4
	117	07-31-10	7.31	29.96	93	151	103	78.1	250	15.4	68.0	99.1	173	379	233	909	891	1.9	-21.9	81.8
	118	07-31-10	7.35	28.4	2	233	84.2	101	323	12.8	84.0	101	203	460	229	1165	1051	9.8	-21.1	94.7
	119	07-31-10	7.67	30.38	93	136	87.8	73.6	231	16.4	64.6	94.4	184	382	226	834	909	-9.1	-20.8	80.5
Rong R.	120	07-30-10	7.57	31.83	68	193	79.1	50.3	146	16.4	192	84.0	31.5	344	309	664	683	-2.8	-20.3	65.8
	121	07-30-10	6.96	30.62	94	509	103	56.1	213	15.9	511	78.5	82.3	379	222	1150	1133	1.5	-20.0	94.4





	Dingjiang	Chayang	11.5	11.802	974	17	6	46	32	0.32	0.18	7.2	26.9	15.4	42.3	275	158	201
Rong		Jieyang	3.11	4.408	706	10	55	11	24	0.05	0.07	2.6	12.0	14.8	26.8	67	152	46
Whole SECRB			270	287	939					5.23	4.90	6.0	18.2	17.1	35.3	222	176	167

<sup>a</sup> Cat<sub>sil</sub> are calculated based on the sum of cations from silicate weathering.

<sup>b</sup> SWR, CWR and TWR represent silicate weathering rates (assuming all dissolved silica is derived from silicate weathering), carbonate weathering rates and total weathering rates, respectively.

<sup>c</sup> CO<sub>2</sub> consumption rate with assumption that all the protons involved in the weathering reaction are provided by carbonic acid.

<sup>d</sup> Estimated CO<sub>2</sub> consumption rate by silicate weathering when H<sub>2</sub>SO<sub>4</sub> originating from acid precipitation is taken into account.

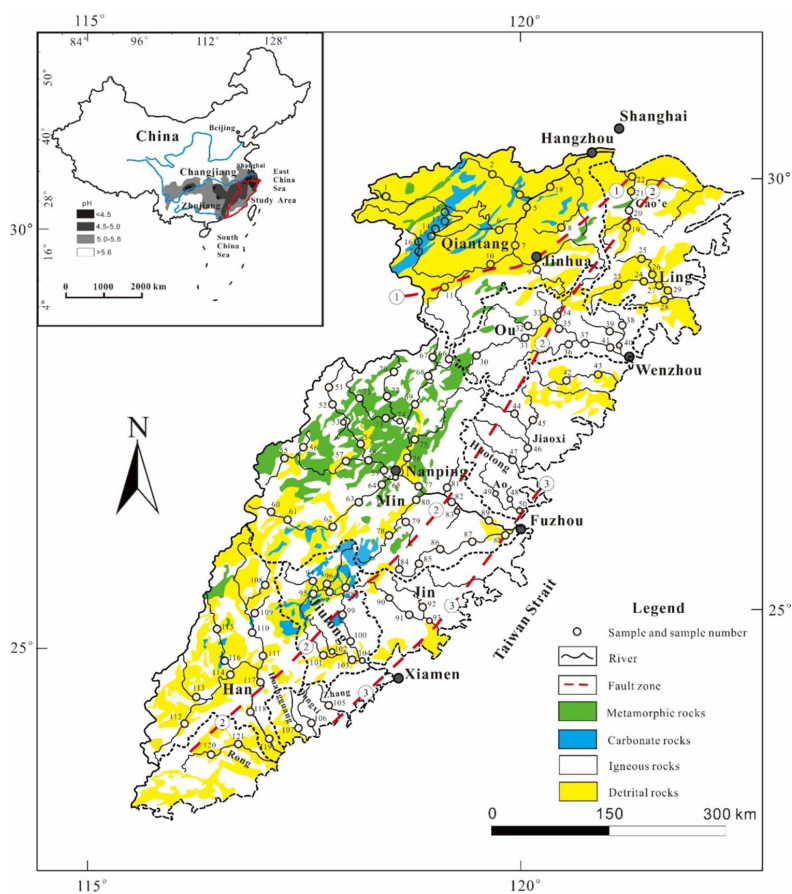


Fig. 1. Sketch map showing the lithology, sampling locations, and sample number of the SECRs drainage basin, and regional rain water pH ranges are shown in the sketch map at the upper-left. (modified from Zhou and Li, 2000; Shu et al., 2009; Xu et al., 2016, rain water acidity distribution of China mainland is from State Environmental Protection Administration of China). ①Shaoxing-Jiangshan fault zone; ②Zhenghe-Dapu fault zone; ③Changle-Nanao fault zone. The figure was created by CorelDraw software version 17.1.

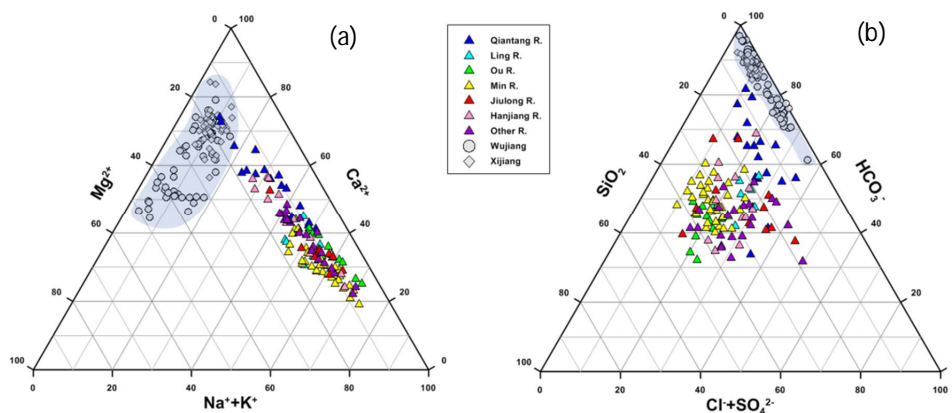


Fig. 2. Ternary diagrams showing cations (a), anions and dissolved  $\text{SiO}_2$  (b) compositions of river waters in the SECRB. Chemical compositions from case studies of rivers draining carbonate rocks are also shown for comparison (data from Han and Liu 2004; Xu and Liu 2007, 2010)

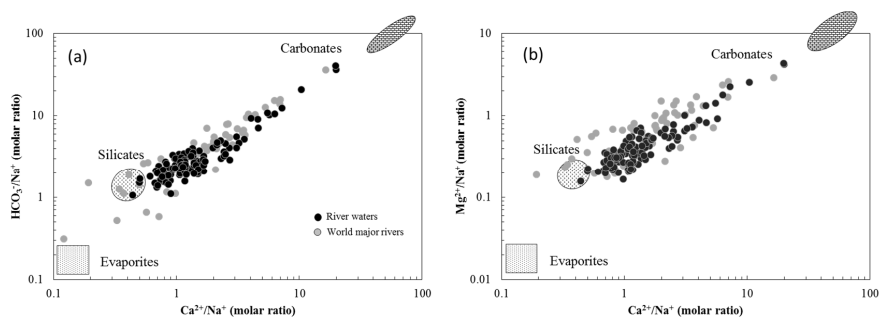


Fig. 3. Mixing diagrams using Na-normalized molar ratios:  $\text{HCO}_3^-/\text{Na}^+$  vs.  $\text{Ca}^{2+}/\text{Na}^+$  (a) and  $\text{Mg}^{2+}/\text{Na}^+$  vs.  $\text{Ca}^{2+}/\text{Na}^+$  (b) for the SECRB, showing a mixing line between silicate and carbonate end-members. Data for world major rivers are also plotted for comparison (data from Gaillardet et al. 1999).

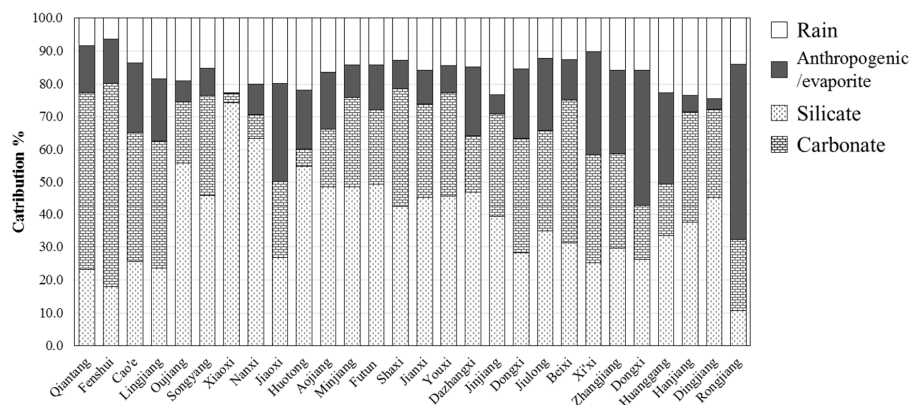


Fig. 4. Calculated contributions (in %) from the different reservoirs to the total cationic load for major rivers and their main tributaries in the SECRB. The cationic load is equal to the sum of  $\text{Na}^+$ ,  $\text{K}^+$ ,  $\text{Ca}^{2+}$  and  $\text{Mg}^{2+}$  from the different reservoirs.

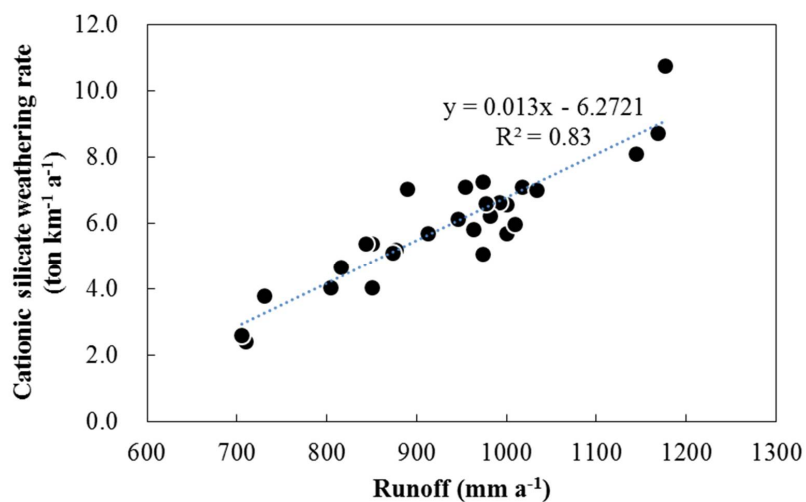


Fig. 5. Plots of the cationic-silicate weathering rate ( $\text{Cat}_{\text{sil}}$ ) vs. runoff for the SECRB, showing that runoff has a strong control on chemical weathering rates of silicates.

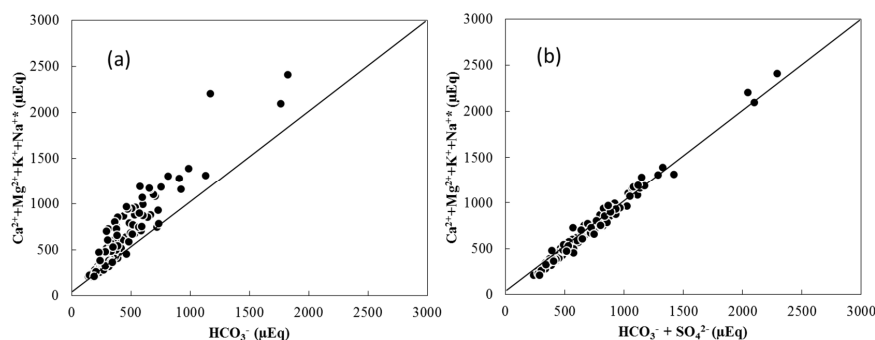


Fig. 6. Plots of total cations derived from carbonate and silicate weathering vs.  $\text{HCO}_3^-$  (a) and  $\text{HCO}_3^- + \text{SO}_4^{2-}$  (b) for river waters in the SECRB.

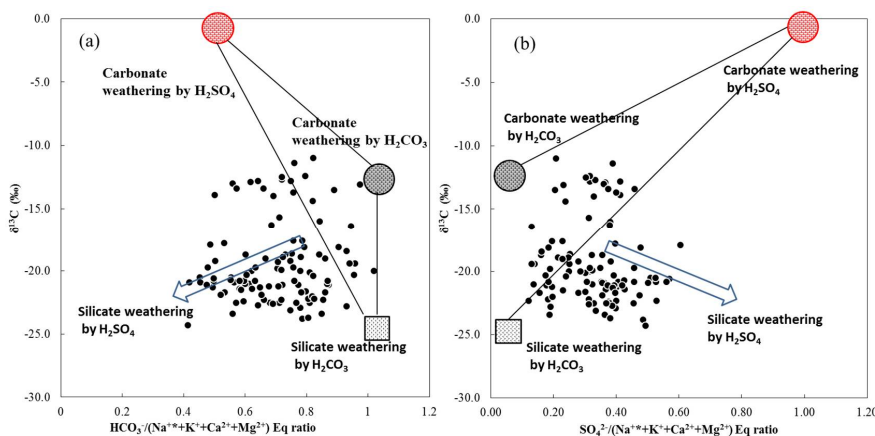


Fig. 7.  $\delta^{13}\text{C}_{\text{DIC}}$  vs.  $\text{HCO}_3^-/(\text{Na}^+ + \text{K}^+ + \text{Ca}^{2+} + \text{Mg}^{2+})$  Eq ratio (a) and  $\text{SO}_4^{2-}/(\text{Na}^+ + \text{K}^+ + \text{Ca}^{2+} + \text{Mg}^{2+})$  Eq ratio (b) in river waters draining the SECRB. The plot show that most waters deviate from the three endmember mixing area (carbonate weathering by carbonic acid and sulfuric acid and silicate weathering by carbonic acid), illustrating the effect of sulfuric acid on silicate weathering.